JOURNAL OF COMPUTATIONAL PHYSICS 41, 142–153 (1981)

TRIDIF, A Triangular Mesh Diffusion Code*

JOHN R. FREEMAN

Sandia National Laboratories, Albuquerque, New Mexico 87185

Received September 11, 1980

A triangular mesh finite difference code designed to study time-dependent magnetic diffusion and eddy current problems is described. TRIDIF is an extension of an existing widely used steady-state magnet design code entitled PANDIRA. The modifications required for the standard PANDIRA difference equations are presented. Sample results include magnetic field distributions in ion diodes and sources used for particle beam fusion applications.

I. INTRODUCTION

The design of conventional dc magnets for plasma physics or high-energy accelerator experiments has relied on large numerical codes which compute the magnetostatic fields produced by specified coil and magnetic material distributions. The more advanced of these have included a capability for treating curved or irregular boundaries [1], variable permeability, and three-dimensional field distributions [2]. Many recent magnet applications require pulsed fields in which metals of high electrical conductivity are used to shape fields. One example is the intense light ion diode experiments [3, 4] being carried out to determine the feasibility of inertial confinement fusion. Another application is in the development of electron-beam pumped gas lasers [5] wherein (for certain designs) pulsed solenoidal guide fields for the electrons must diffuse around massive metal drift tube supports. Smooth field profiles are required for uniform excitation of the lasing medium. These applications require numerical codes with most of the sophistication of the conventional magnet codes, plus the capability for including the time-dependent diffusion of the magnetic flux and the eddy currents in the surrounding media. We describe here a triangular mesh diffusion code called TRIDIF which attempts to provide such a tool.

TRIDIF is basically a modification to include time-dependence of an existing static magnet design code entitled PANDIRA. PANDIRA is a widely used triangular mesh finite difference code which solves a Poisson equation for the magnetic vector potential by means of a direct matrix inversion. SUPERFISH, a version of the code

* Work supported by the U.S. Department of Energy under Contract DE-AC04-76-DP00789.

0021-9991/81/050142-12$02.00/0

for studying the mathematically similar problem of rf cavity excitation, has been discussed by Halbach and Holsinger [6]. PANDIRA is a direct descendent of the original TRIM code published by Winslow [1] in 1966 and thus reflects considerable development and refinement by the high-energy accelerator magnet design community. An intermediate version of the code (called POISSON), also in wide use, employed successive overrelaxation (SOR) to solve the field equation.

Winslow's original paper [1] used a time-dependent diffusion equation to develop the difference equations for the static field class of problems. Despite this, all of the applications in Ref. [1] and all of the subsequent publications using the various evolutionary versions of the code were restricted to static field problems. Halbach [7] published an interesting paper on eddy-current effects in accelerator magnets which used a number of simplifying assumptions to show qualitative effects, but again used the static version of the code. The present work describes a method for converting PANDIRA into a time-dependent code for magnetic diffusion and eddy current calculations.

The PANDIRA code and its predecessors provide a very attractive basic module. The triangular mesh gives an excellent definition of curved and irregular surfaces. Fine zoning can be added easily where good resolution is required. An automatic mesh generator greatly reduces the difficulty of coping with the triangular mesh. The user need only specify the zoning along the exterior boundary and selected interior interfaces; the mesh generator [1] then solves a Laplace equation for the interior mesh point locations.

The early versions of the code, such as TRIM and POISSON, relied on an accelerated SOR iterative method. We have found that for time-dependent problems, where many hundreds of time-steps might be required, the direct matrix solver of the later versions of the code [6] provides the speed and stability required. In early studies of the present work which used meshes of greatly varying density in both coordinates, convergence using the SOR version was frequently slow and sometimes not achieved at all. The direct solver, by contrast, always gives an exact solution to the difference equation with a speed which is independent of the mesh distribution.

Other approaches to solving time-dependent field diffusion problems have been based on an integral equation method [8–12] in which the conductors are modeled by triangular finite elements. The field at any point is related to the distributed eddy currents by means of an inductance matrix whose elements involve integrations over the triangular cross sections. Advantages of this method are that vacuum regions need not be discretized and that no external boundary conditions are required. A disadvantage is that the inductance matrix is non-sparse, so that only a limited number of elements can be used in practical problems.

In Section II, the modifications to the difference equations are presented and the new structure for time-dependent problems is discussed. Section III presents results for sample problems. This work is summarized in Section IV.

II. Method of Solution

The usual equation which describes the diffusion of the magnetic vector potential $\hat{A}$, where the magnetic field $\hat{B} = \nabla \times \hat{A}$, is given by

$$\mu_0 \sigma \frac{\partial \hat{A}}{\partial t} = -\nabla \times \nabla \times \hat{A} + \mu_0 \hat{J}_s, \tag{2.1}$$

where J_s is a source current density produced within the magnet coils, μ_0 is the permeability of free space and σ is the electrical conductivity. For the present derivation and applications, all materials are assumed to have a simple constant free space permeability; the extension to magnetic materials appears fairly straightforward, but no problems have thus far been attempted. In vacuum regions where $\sigma = 0$, Eq. (2.1) is seen to reduce to the usual static equation,

$$\nabla \times \nabla \times \hat{A} = \mu_0 \hat{J}_s. \tag{2.2}$$

For azimuthally symmetric problems in cylindrical coordinates with $\hat{J}_s = J_{s\theta}\hat{\theta}$, the magnetic stream function $\psi = rA_\theta$ is generally used, and Eq. (2.1) becomes

$$\frac{\mu_0 \sigma}{r} \frac{\partial \psi}{\partial t} = \frac{\partial}{\partial r}\left(\frac{1}{r}\frac{\partial \psi}{\partial r}\right) + \frac{\partial}{\partial z}\left(\frac{1}{r}\frac{\partial \psi}{\partial z}\right) + \mu_0 J_{s\theta}, \tag{2.3}$$

the magnetic field components are given by

$$B_z = \frac{1}{r}\frac{\partial \psi}{\partial r} \qquad \text{and} \qquad B_r = -\frac{1}{r}\frac{\partial \psi}{\partial z}.$$

The mesh chosen by Winslow [1] uses exactly six nearest neighbors, as shown in Fig. 1. There is no restriction required on the shape of the triangles. Equation (2.3) is differenced as

$$\frac{G_j(\psi_j^{n+1} - \psi_j^n)}{\Delta t} = \sum_{i=1}^{6} W_i(\psi_i^{n+1} - \psi_j^{n+1}) + S_j^{n+1}, \tag{2.4}$$

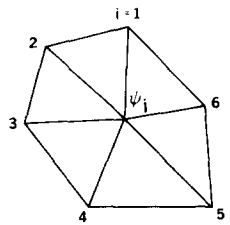

Fig. 1. Basic module of triangular mesh.

where the superscript n refers to the time differencing and the summation on the right-hand side is taken only over the six nearest neighbors. The weights W_i are coupling coefficients which depend only on the geometry of the triangles. The term $S_j^{n+1} = (\mu_0/3) \sum_{i=1}^{6} J_{s\theta_{i+1/2}}^{n+1} A_{i+1/2}$, where $A_{i+1/2}$ is the area of the triangles, is proportional to the total source current contained within the mesh volume centered at point j. This represents the coil source current assumed to be specified for all time as input. The remaining quantity $G_j = 1/3 \sum_i (\mu_0 \sigma_{i+1/2}/r_j) A_{i+1/2}$ is proportional to the electrical conductance at the mesh location. For this treatment, it is assumed that σ, the electrical conductivity, is an arbitrary function of space but is independent of time. As seen from Eq. (2.4), the equation is time differenced fully implicitly, with the spatial differencing centered at t^{n+1}. This has the advantage of good stability and, more importantly, requires fewer modifications than a time-centered differencing. The penalty paid, however, is a time differencing which is accurate in Δt to first, rather than second, order.

Equation (2.4) can be rewritten as

$$\psi_j^{n+1} = \frac{\sum_i W_i \psi_i^{n+1} + S_j^{n+1} + \psi_j^n G_j/\Delta t}{\sum_i W_i + G_j/\Delta t}. \tag{2.5}$$

(If $G = 0$, this reduces identically to the static case difference equation of Winslow.) At each time step Eq. (2.5) is solved using the direct matrix method for the new ψ_j^{n+1}. The only changes required to the existing PANDIRA program are to have stored the ψ_j^n from the preceding time step and the G_j, which need to be computed and stored only once just after the mesh generation section, since these coefficients are time-independent. The present code structure already exists to sum the $J_{s\theta}$ over the triangles to compute S_j so that only slight additions are required to also obtain the G_j over the whole mesh. For the examples to be presented, the time step was limited to the value used for most explicit calculations, namely, $\Delta t \simeq 0.4 \mu_0 \sigma \Delta^2$, where Δ is the smallest Δr or Δz found in metallic regions. More recent computations have used a variable time-step based on limiting the maximum change of any ψ_j to a few percent per time step. Some care must be exercised with this type of time step control for applications which require high accuracy of small magnetic field components. since some accuracy will be lost in performing the required numerical differentiation of the ψ_j values.

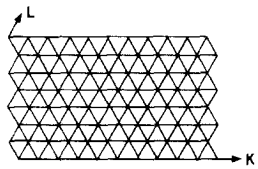

FIG. 2. Portion of logical mesh used to define problem. The mesh generator converts this to an optimized mesh of variable shape and density.

PANDIRA uses a logical mesh to identify each mesh point with a label K and L, shown in Fig. 2. (In this notation the ψ_j^n in the preceding equations become ψ_{LK}^n, S_j^{n+1} becomes S_{LK}^{n+1}, etc.) The mesh generator produces a topologically equivalent physical mesh, but one in which all boundaries are defined by mesh lines. With this indexing, Eq. (2.5) can be rewritten as [6]

$$\begin{bmatrix} a_{11} & a_{12} & & & & \\ a_{21} & a_{22} & a_{23} & & & \\ & a_{32} & \vdots & & & \\ & & & a_{L_2-1,L_2-2} & a_{L_2-1,L_2-1} & a_{L_2-1,L_2} \\ & & & & a_{L_2,L_2-1} & a_{L_2,L_2} \end{bmatrix} \begin{bmatrix} \Psi_1 \\ \Psi_2 \\ \vdots \\ \Psi_{L_2-1} \\ \Psi_{L_2} \end{bmatrix} = \begin{bmatrix} S_1 \\ S_2 \\ \vdots \\ S_{L_2-1} \\ S_{L_2} \end{bmatrix}, \tag{2.6}$$

where K_2 is the maximum value of K and L_2 is the maximum value of L.

The matrix A on the left-hand side of Eq. (2.6) is a block tridiagonal matrix as shown; each block is itself sparse with only three nonzero elements per row. Each element of Ψ_L is a vector with components ψ_{LK}^{n+1}, for $K = 1$ to K_2. The elements of the right-hand side are vectors with elements $S_{LK}^{n+1} + \psi_{LK}^n G_{LK}/\Delta t$, for $K = 1$ to K_2, i.e., the standard PANDIRA source array modified by the addition of one of the extra terms shown in Eq. (2.5); the only other modification is made to the diagonal matrices a_{ii}, where the central elements $(\sum_i W_i)_{LK}$ become $(\sum_i W_i + G_j/\Delta t)_{LK}$. The Gaussian block elimination and back substitution for the solution then takes place as described in Ref. [6].

III. Sample Applications

TRIDIF was initially applied to a series of test problems with variations in one dimension only for which analytic or previous numerical results were available. These included 1-D cartesian or cylindrical field diffusion in homogeneous media and the diffusion of infinite length cylindrical solenoid fields into a cylindrical metal annulus. Results for both Neumann and Dirichlet boundary conditions were obtained satisfactorily.

The first two-dimensional case studied was the field configuration for an intense pulsed cylindrical ion diode [3] in which a field transverse to the diode electrodes is used to inhibit the electron current. These fields are established over a time scale of many microseconds prior to initiation of the high-voltage pulse (~50 nsec) which accelerates the ions. The field is produced by two coils, as shown in Fig. 3. The skin depth in the aluminum anode is a few millimeters so that the field approximately follows the contour of the surface, which is shaped to focus the ion beam to a spot on the axis. Field diffusion into the anode is undesirable, since the ions will be emitted with a significant canonical angular momentum which will reduce the focusability of the diode. To reduce the flux diffusion, the current coils are driven first with a slow low-amplitude negative pulse (one-quarter of a sinusoid, quarter period ~1 msec)

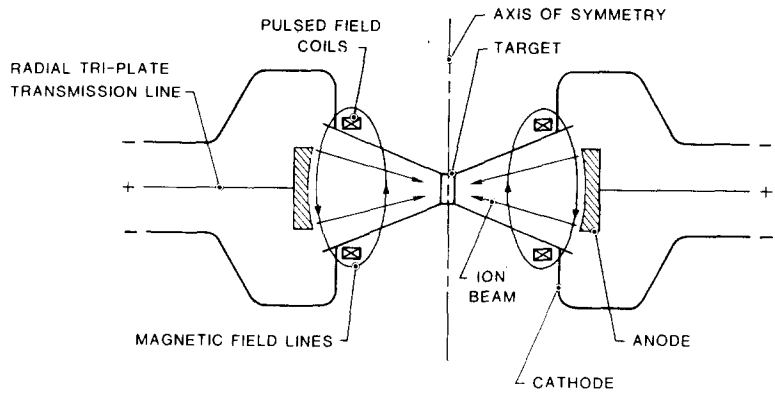

FIG. 3. Schematic configuration of pulsed cylindrical ion diode used for particle beam fusion experiments. The field coils are used to prevent direct electron flow from the cathode to the anode. Typical parameters are an anode radius of 5–15 cm, voltage of 1–2 MV, power of 0.1–1.0 TW, and a beam pulse length of 50 nsec.

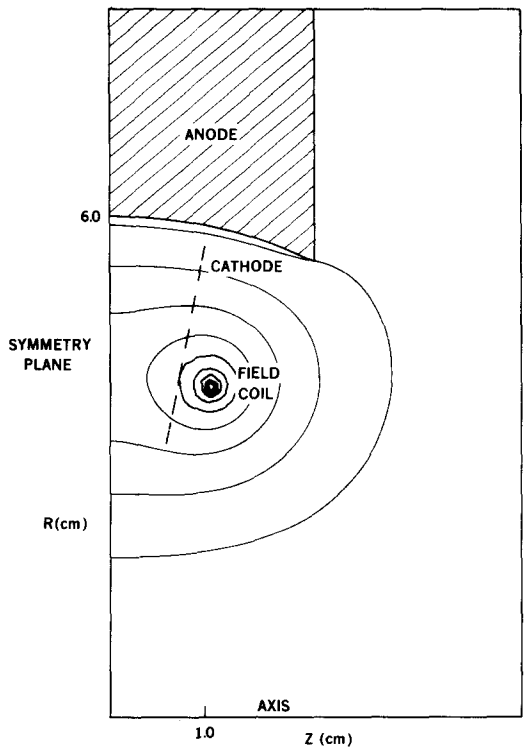

FIG. 4. Diode configuration for studying effect of anode curvature. Electrons from the cathode blades are forced to follow magnetic field lines, forming a virtual cathode near the central portion of the anode ($z = 0$). Ions are emitted at the anode and accelerated radially inward to a central target. The computed field lines at the peak of the initial slow current pulse are shown.

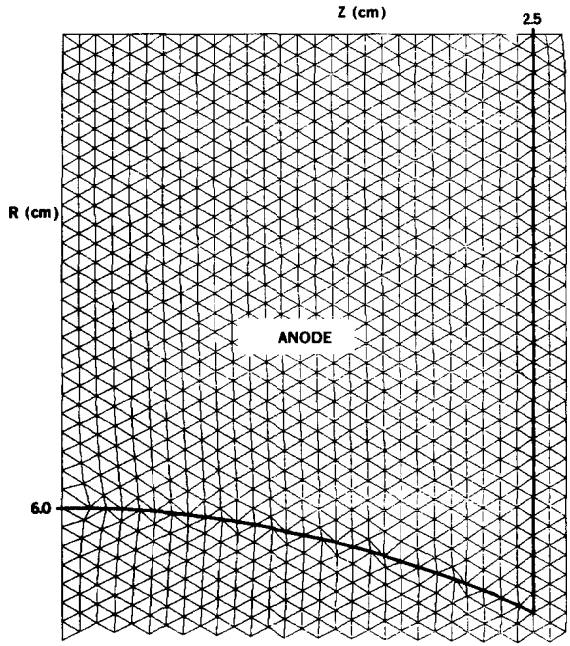

FIG. 5. Expanded view of the computational mesh in the region of the anode emission surface.

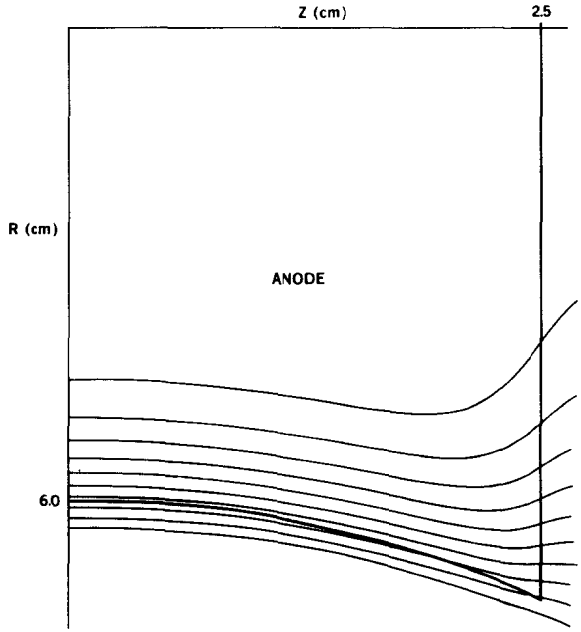

FIG. 6. Expanded view of the field lines near the anode surface at the peak of the initial slow current pulse.

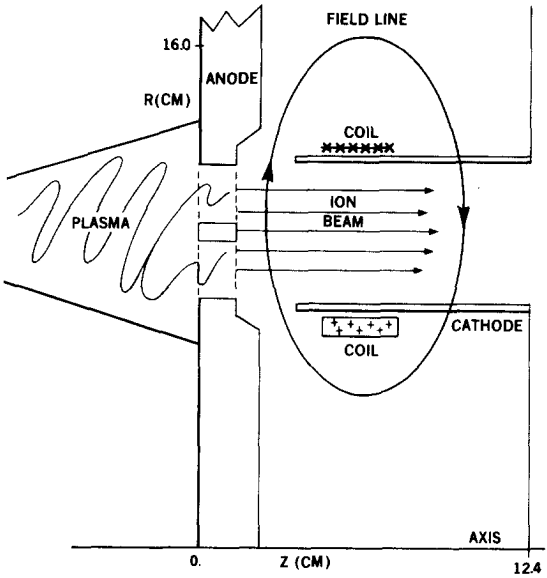

FIG. 7. Configuration for the Pulselac linear accelerator problem. An annular beam of ions is extracted from the plasma gun source region by a voltage applied to the cathode. The magnetic field is used to control the electron flow and to focus the ions.

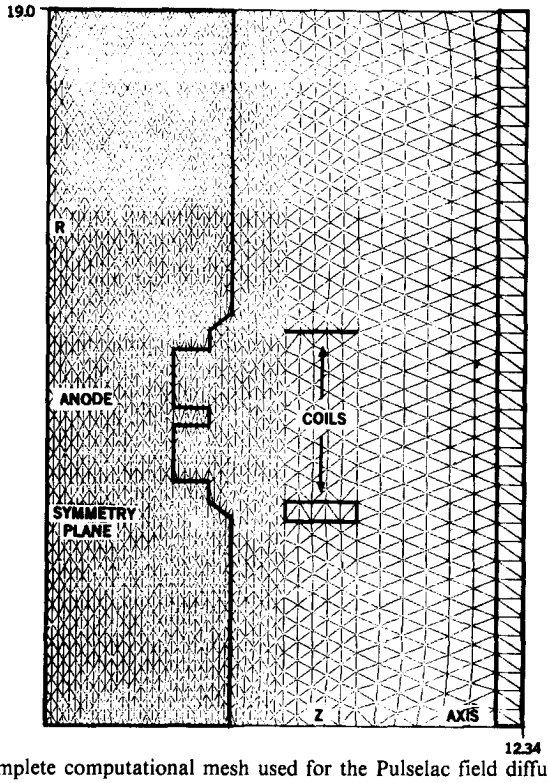

FIG. 8. Complete computational mesh used for the Pulselac field diffusion solution.

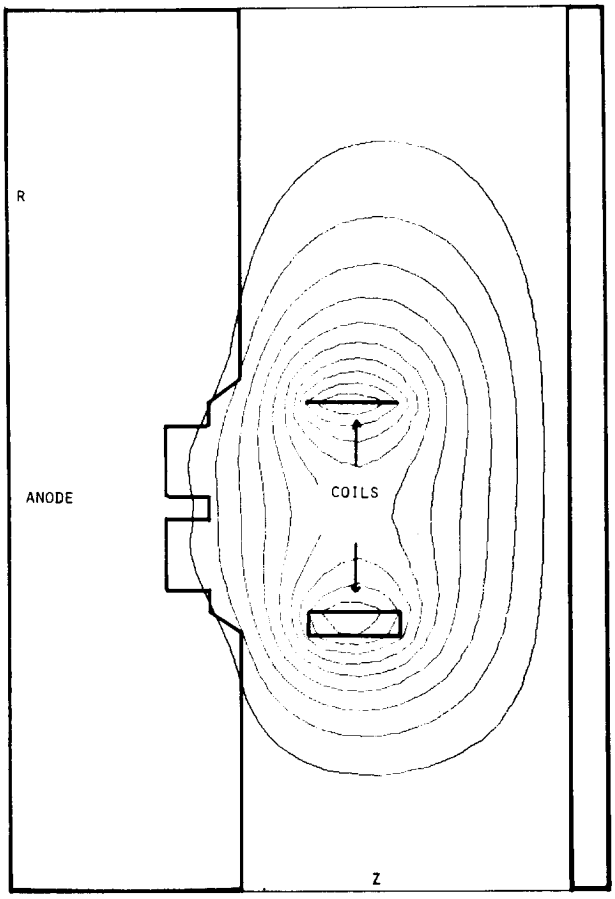

FIG. 9. Magnetic field distribution at the peak of the current pulse.

followed by a fast high-amplitude positive pulse. The net effect is to greatly reduce the trapped flux when the ion beam is formed.

Figure 4 shows the computed field lines at peak curent in the TRIDIF calculation of the initial slow reverse field distribution. An expanded view of the computational mesh near the anode, which for this early study was of uniform density, is shown in Fig. 5. The excellent resolution of the surface curvature is evident. The stream function (field lines) in the anode at the time of peak current are shown in Fig. 6, which shows the same spatial region as Fig. 5. Figures 4 and 6 show the field lines in different regions of the mesh at the same point in time. About 50 time steps were required for this solution.

A more challenging application of the code was the study of a new ion injector configuration, shown in Fig. 7, for Pulselac [4], a multistage linear ion accelerator for inertial confinement fusion. The basic physics is similar to that of the external field

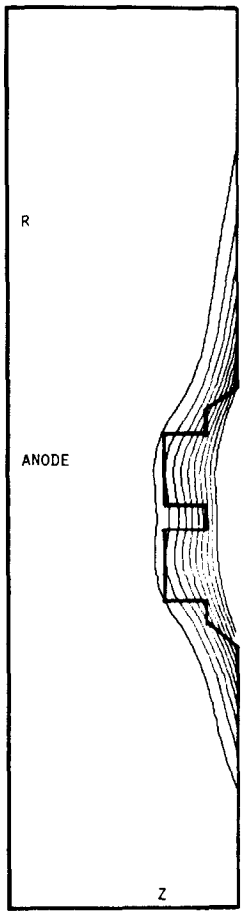

FIG. 10. Expanded view of the field lines at the emission region of the anode.

control diode of Fig. 3; in this case pulsed magnetic fields are used to inhibit electron flow, to enhance the ion emission rate and to focus the resultant beam. A separate plasma source is used to provide a supply of ions. The exact shape of the field lines at the anode is crucial for controlling electron loss and the initial beam emittance. The axis of symmetry in Fig. 7 is at the bottom of the figure. The ions which are to be injected into the accelerator are thus in the form of an annular beam. The anode material was again aluminum and the right-hand boundary was modeled as a perfectly conducting plane. Figure 8 shows the complete computational mesh. The streamlines at the time of peak current ($t \simeq 0.07$ msec) are shown in Fig. 9. Figure 10 shows the field lines near the ion source with greater resolution. The flexibility of the code allowed the study of a variety of anode shapes to optimize the fields for controlling the electrons.

The most recent application of the code was the study of field diffusion around

supports in an electron-beam pumped gas laser [5]. Smooth field profiles are desired to obtain uniform excitation of the lasing medium. Eddy currents induced in the supports lead to potentially damaging field perturbations. To test the predictions of the code, two coils were arranged in the Helmholtz configuration to produce a pulsed cylindrical field volume. Two annular stainless steel slugs were inserted to represent the laser cavity support rings. The spatial and temporal behavior of the magnetic fields were measured with Rogowski loops and compared with the computed fields. The fields compared to better than 10% for all positions and times for which data was taken. The details of this work are available in Ref. [13].

IV. Summary

A code for computing pulsed magnetic field diffusion problems has been constructed by making modest modifications to the existing PANDIRA code, which was written for static problems. The triangular mesh and automatic zoner provide great geometric flexibility while the direct matrix solver provides the speed required for practical time-dependent problems. The speed of the solver per time step was found to be equivalent to that claimed in Ref. [6], namely, $T_c = T_1 N^2 \varepsilon$, where T_c is the CPU time, N is the total number of logical mesh points, and ε is the smaller of K_2/L_2 or L_2/K_2. For CDC-7600, $T_1 \simeq 0.75\,\mu$sec. A significant increase in speed should be possible by storing some of the time-invariant matrices. This type of code should also be of use for many other physical problems, such as thermal diffusion.

Acknowledgments

The significant task of adapting PANDIRA to the Sandia computer system was completed by Ronald Hadley. Ronald Holsinger kindly provided us with a copy of the code and contributed invaluable assistance with its adaptation. Helpful discussions were held with Stanley L. Humphries, Jr., David J. Johnson, and Edward L. Patterson.

References

1. A. M. Winslow, *J. Comput. Phys.* **1** (1966), 149.
2. A. G. Armstrong, C. J. Collis, N. J. Diserens, M. J. Newman, J. Simkin, and C. W. Trowbridge, "GFUN3D User Guide," Report RL-76-291A, Rutherford Laboratory, 1976.
3. D. J. Johnson, G. W. Kuswa, A. V. Farnsworth, JR., J. P. Quintenz, R. J. Leeper, E. J. T. Burns, and S. Humphries, Jr., *Phys. Rev. Lett.* **42** (1979), 610.
4. S. Humphries, Jr., G. W. Kuswa, C. W. Mendel, and J. W. Poukey, *IEEE Trans. Nucl. Sci.* **NS-26** (1979), 4220.
5. J. J. Ramirez, *in* "Proceedings, Fourteenth Pulse Power Modulator Symposium, Orlando, Florida, June 1980."
6. K. Halbach and R. F. Holsinger, *Particle Accel.* 7 (1976), 213.
7. K. Halbach, *Nucl. Instrum. Meth.* **107** (1973), 529.

8. C. S. BIDDLECOMBE, C. J. COLLIE, J. SIMKIN, AND C. W. TROWBRIDGE, *in* "Proceedings, COMPUMAG Conference on the Computation of Magnetic Fields, Oxford, 1976.
9. C. S. BIDDLECOMBE, *in* "Proceedings, COMPUMAG Conference on the Computation of Magnetic Fields, Grenoble, 1978."
10. L. R. TURNER, *IEEE Trans. Mag.* **MAG-113** (1978), 1119.
11. L. R. TURNER AND R. J. LARI, *in* "Proceedings, COMPUMAG Conference on the Computation of Magnetic Fields, Grenoble, 1978."
12. L. R. TURNER, R.J. LARI, AND G. L. SANDY, *in* "Proceedings, Symposium on Eddy Current Characterizations of Materials and Structures, Gaithersberg, 1979."
13. E. L. PATTERSON AND J. R. FREEMAN, "Pulsed Magnetic Field Distribution Near Conducting Rings," SAND80-1546, Sandia National Laboratories, 1980.